Efficient multiphysics modeling of microelectromechanical switches

Yongjae Lee[1] and Dejan S. Filipovic[1]
[1]Engineering Center, ECOT 243, 425 UCB, University of Colorado, Boulder, CO 80309-0425
yongjae@ieee.org and dejan@colorado.edu

ABSTRACT

Circuit simulations driven modeling approach with embedded multi-physics of capacitive radio frequency microelectromechanical systems switches is presented in this paper. Finite element method simulations in electromagnetic, electromagnetic-thermal and thermal-stress domains are sequentially performed to model and capture the behavioral phenomenology inherent to the selected device. Computed effects are then utilized to modify the original electromagnetic model, giving rise to the updated solutions with included electromagnetic-thermal-stress-electromagnetic physics. To enable circuit level design with the multi-physics models of capacitive microelectromechanical switches, an artificial neural network technique is utilized. Compared to the finite element method simulations, the developed neural network models are about 1500 times faster while maintaining smaller than 0.5% relative difference. Finally, these models are integrated in a circuit simulator, where the sensitivity study and optimization are performed to further demonstrate the advantages of the proposed modeling approach.

1. INTRODUCTION

Over the past decade, a significant progress in the design, fabrication, and application of radio frequency microelectromechanical system (RF MEMS) switches has been reported. Small size, low power consumption, low loss and high isolation are typical advantages of these devices when compared to traditional switches [1]–[2]. Once desired reliability and manufacturing costs are achieved, a widespread implementation in current and future high performance wireless communication systems will become feasible. In this paper, we propose a modeling approach that includes coupled electromagnetic (EM)-thermal and thermal-stress effects on the RF performance of capacitive MEMS switches and also allows for the device and system level design and optimization. Coupled EM-thermal analysis and measurement techniques have been reported in the past [3], [4] and applied for the RF characterization of MEMS switches [5]. Excellent prediction capabilities are demonstrated with coupled finite element method (FEM) [6]–[9] and finite difference [5], [10] based electro-thermal analysis. However, these techniques are formulated for the device level simulations and owing to the numerical solution of the partial differential kernel, they impose some memory restrictions and require longer running time. Improved computational efficiency and circuit level simulations are obtained with analytical [11] or equivalent circuit models [12], [13]. Although fast, these approaches often fail to accurately model more

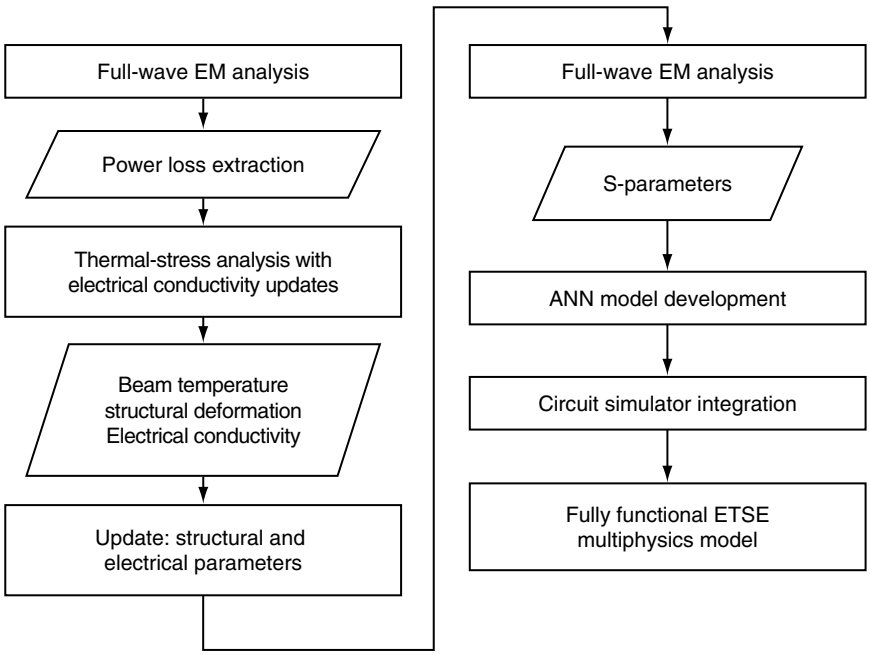

Figure 1 Flowchart of the circuit level multi-physics modeling methodology for RF MEMS switches.

complex structures and related coupled effects. To alleviate these limitations, a circuit level design and optimization methodology for RF MEMS switches using artificial neural network (ANN) technique is proposed. Utility of ANN for EM-only modeling was reported in our earlier work [14]. Here, the methodology is extended to account for multi-physics operation of a coplanar waveguide (CPW) MEMS shunt switch reported in [15]. A high-level flowchart description for the proposed approach is given in Figure 1.

Specifically, the algorithm starts with an EM solver, Ansoft's HFSS [16], and computation of the dissipated power on the switch beam. Computed surface power loss distribution is imported to Ansoft's ePhysics [17] where the temperature distribution is evaluated. Structural deformation, specifically, the beam deflection due to the temperature rise is also computed. Next, the beam deflection profile and reduced electrical conductivity changes are used to update the original EM model. Finally, S-parameters are computed in HFSS. The updated EM model embraces the first order electromagnetic- thermal-stress effects and higher orders can be obtained by repeating the same sequence of steps. Once the validity of EM-thermal and thermal-stress analyses are demonstrated, a "blackbox" artificial neural network (ANN) model for the switch is developed using the datasets generated from these EM-thermal-stress-EM simulations. Additional functionalities and versatilities of multi-physics ANN models are demonstrated by facilitating their integration in the circuit simulator, Agilent's ADS [18]. Although proposed modeling approach requires extensive time and effort for developing ANN models, once they are developed, circuit level design, analysis, and optimization of MEMS switches and circuits with embedded black-box models of these devices can be conveniently conducted within the circuit simulator environment. Along with the enabled functionality, the significant savings in time are also obtained.

Although the developed models might not include all mechanisms associated with this type of MEMS switches, it is noted that the proposed modeling methodology provides a promising viable way for CAD engineering of RF circuits with MEMS devices.

This paper is organized as follows. EM-thermal and thermal-stress models of the CPW MEMS shunt switch are described and validated in Section 2. In Section 3, multi-physics effects on the RF performances of a switch are demonstrated. Section 4 describes the development of multi-physics ANN models. The sensitivity analysis using the developed ANN models is performed in Section 5. In Section 6, the ANN models are integrated in the circuit simulator and simple optimization examples are described. Finally, the convergence study and the accuracy of the developed EM-thermal-stress-EM models are discussed in Section 7.

2. NUMERICAL MODELS

In this section, EM-thermal and thermal-stress models of a MEMS switch are developed and compared with available numerical and analytical reference data. Presented results demonstrate high accuracy of multi-physics FEM models, which form a baseline for the development of circuit simulator compatible models. Note that the EM model only of the shunt switch was validated with measurements in [14].

2.1. ELECTROMAGNETIC-THERMAL MODEL

Figure 2 shows a simplified drawing of the CPW MEMS shunt switch. Geometrical and thermal parameters of the baseline structure are given in Table 1.

As an RF signal propagates through the CPW transmission line, a current is induced in the switch beam. Due to the non-zero shunt resistance, power is dissipated and resistive heating occurs. The FEM electro-thermal software, ePhysics [17] is utilized to compute the temperature rise in the beam. As seen in Figure 3, excellent agreement between our simulations and literature is obtained for both beam positions.

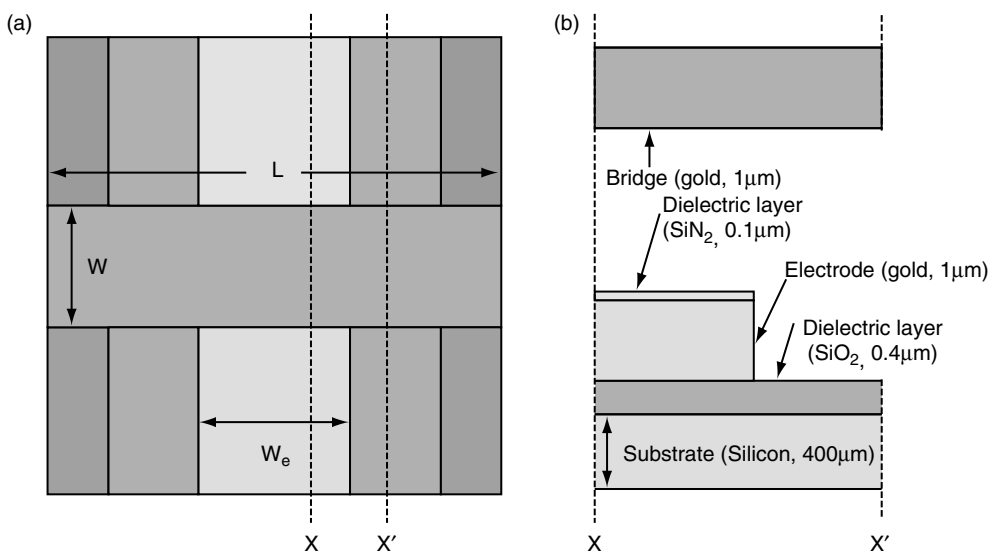

Figure 2 Schematic of a CPW MEMS shunt switch:(a) top view, (b) cross section view between X and X'.

Table 1 Parameters for the baseline CPW MEMS shunt switch [15]

Parameter	Value
Thermal conductivity of gold, λ_{Au} [W/m·K]	315
Young's modulus, E [Gpa]	80
Beam length, L [μm]	300
Beam width, W [μm]	80
Gap, G [μm]	2.5
Beam thickness, t [μm]	1
Electrode width, W_e [μm]	100
Thermal expansion coefficient, α [1/K]	1.4×10^{-5}
Poisson's ratio, ν	0.4
Temperature, T [K]	-

2.2. THERMAL-STRESS MODEL

Due to the temperature rise in the beam and zero displacement boundary conditions applied to the both ends of the beam, the membrane deflects in the vertical direction. This mechanical deflection is calculated in ePhysics and obtained result is compared with analytical expression from [19]. As shown in Figure 4, excellent agreement between our simulations and analytical results with relative error below 4% demonstrate the utility of this tool for modeling important (for this work) coupled thermal-stress effects. Note that a constant temperature distribution along the beam thickness is assumed in this analysis.

3. MULTI-PHYSICS EFFECTS

In this section, the EM-thermal-stress-EM effects on the RF performance are demonstrated. It is clearly shown that these effects should be included for the development of accurate RF models of capacitive MEMS switches. Current induced thermal-stress effects are used to update the original HFSS model (conductivity and geometry) and compute the resultant RF performance. Note that the change of electrical conductivity due to the temperature rise in the beam follows Wiedemann-Franz law [20] ($\sigma = \lambda_{Au}/L_oT$) where L_o is the Lorentz number ($L_o = 2.3 \times 10^{-8}$ WΩ/K). The beam width and gap are W=160μm; G=2.0μm, while other parameters are as in Figure 2 and Table 1.

As seen in Figure 5, noticeable changes in both return loss and insertion loss are observed for the up-state position. For example, at 40GHz, the return loss deteriorates from 6.6dB to 4.6dB while the insertion loss is increased from 1.1dB to 1.8dB. Given in the same plot is the electromagnetic-thermal effect only. As shown, the reduced electrical conductivity of the beam does not significantly contribute to the change of RF performances and the beam deflection dominates. The computed steady state peak temperature of the beam is 244°C.

For the down-state position, the temperature rise contributes only to the change of electrical conductivity. In other words, beam deformation has already occurred and in the RF sense, is final. Figure 6 compares the return and insertion losses before and after the electromagnetic-thermal-electromagnetic effect. As seen, the thermal effect is negligible even if the beam temperature rise is as high as 300°C. The difference in return loss varies from 0.01dB at 1GHz to 0.03dB at 40GHz while the isolation difference is 0.03dB at 1GHz and 0.08dB at 40GHz. For this reason, the developed models for the beam in the down-state position will have embedded only the EM physics.

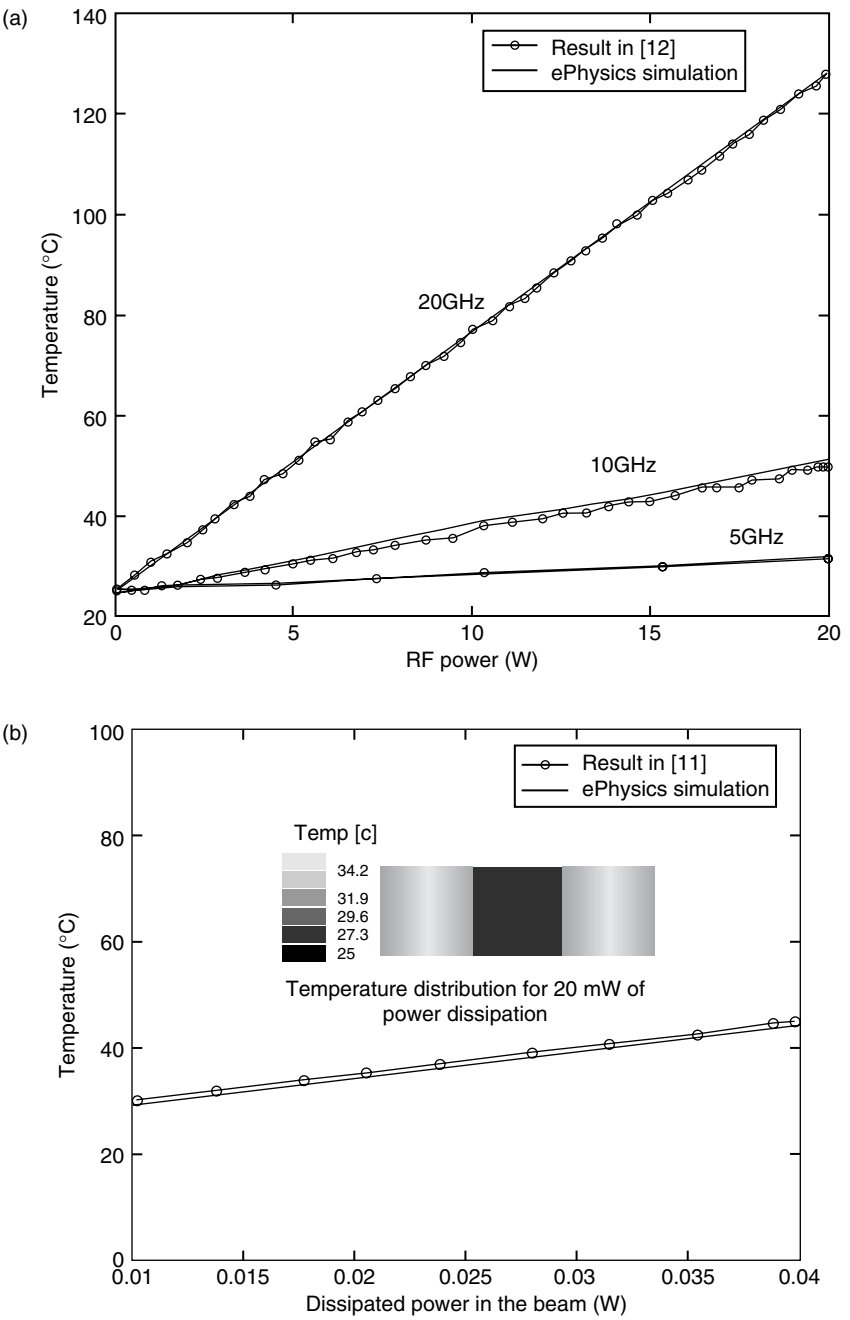

Figure 3 Validation of the EM-thermal model for (a) up-state position; and (b) down-state position. Inset in (b) shows the temperature distribution for 20mW dissipated power on the beam.

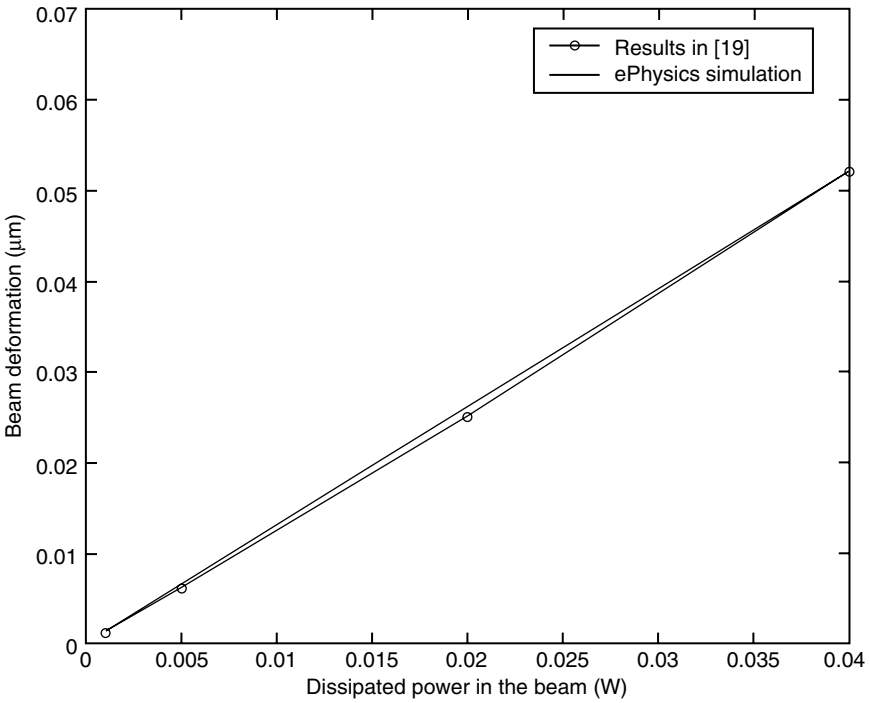

Figure 4 Comparison between the FEM thermal-stress and analytical models for the beam in the up-state position.

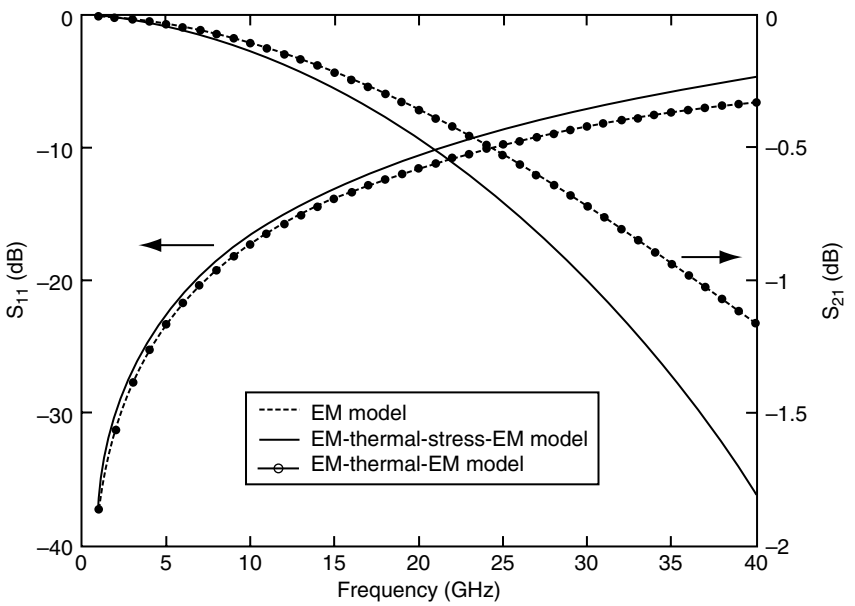

Figure 5 Comparison between EM, EM-thermal-EM, and EM-thermal-stress- EM effects for the beam in the up-state position.

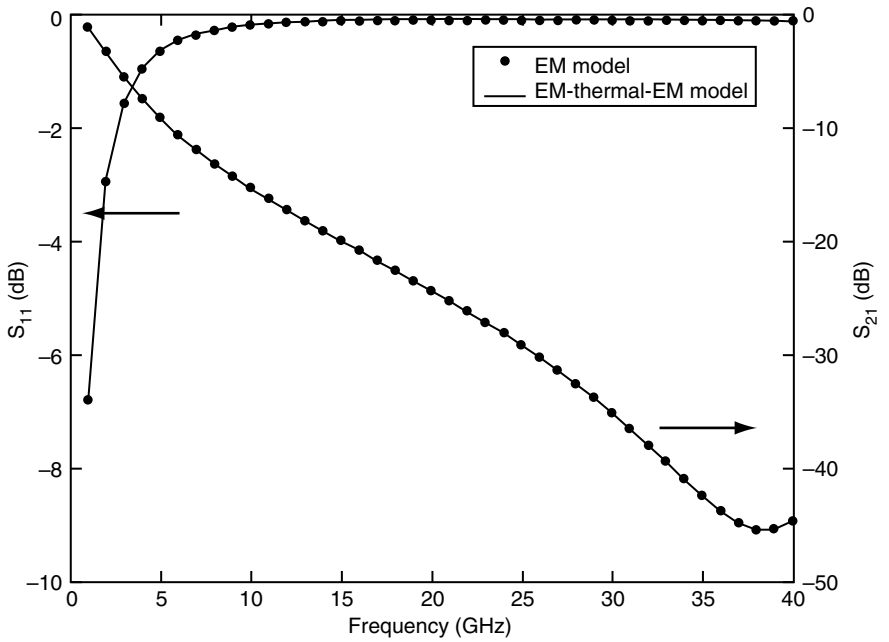

Figure 6 Comparison between EM and EM-thermal-EM effects for the beam in the down-state position.

4. ANN MODEL

In this section, the multi-physics ANN model of a capacitive RF MEMS switches is developed. As depicted in Figure 1, after the EM, EM-thermal, and thermal-stress models are validated, the EM-simulations including thermal-stress and electrical effects are performed to generate ANN datasets. Selected input variables include beam width (W), gap between the CPW center conductor and the beam (G), and magnitude of RF power (P). Output variables are frequency dependent real and imaginary parts of S-parameters. Note that other physical input and output parameters can be also included in the model development, but they have not been considered here due to the longer training time. As demonstrated in the previous section, for the down-state position, important input variables are only the beam width and the gap because from the electrical perspective, no mechanical changes are possible once the switch is closed. Also, the changes in electrical conductivity are almost insignificant and will not be considered.

Given in Table 2 are selected ranges of input parameters for both beam positions. For the up-state position, a total of 45 training and 15 testing datasets are generated while 15 training and 5 testing sets are generated for the down-state position. The ANN architecture is selected following the same procedure as in [21]. For the up-state position, it consists of two-hidden layers with 6 neurons per each layer while two-hidden layers with 3 neurons per each layer are selected for the down-state position. Note that testing of the ANN model is performed with arbitrarily selected input variables, which are different than datasets used for training. In this way, generalization capability is maintained [22]. The correlation coefficients in the excess of 0.99 are obtained for both beam positions.

Validation of the ANN models for three different switch configurations is depicted in Figure 7. Excellent agreement with the numerical EM-thermal-stress-EM and EM FEM models is obtained for the beam in the up and down state position, respectively. Maximum relative error is below 0.5%.

Table 2 Range selection for the input variables of the ANN model

Input variables	Range	Increment (Δ)	Unit	Switch position
Switch sidth	40~160	30	μm	Up and Down
Gap(Beam height)	2~5	1.5	μm	Up and Down
RF power	0.1~1	0.45	Watt	Up

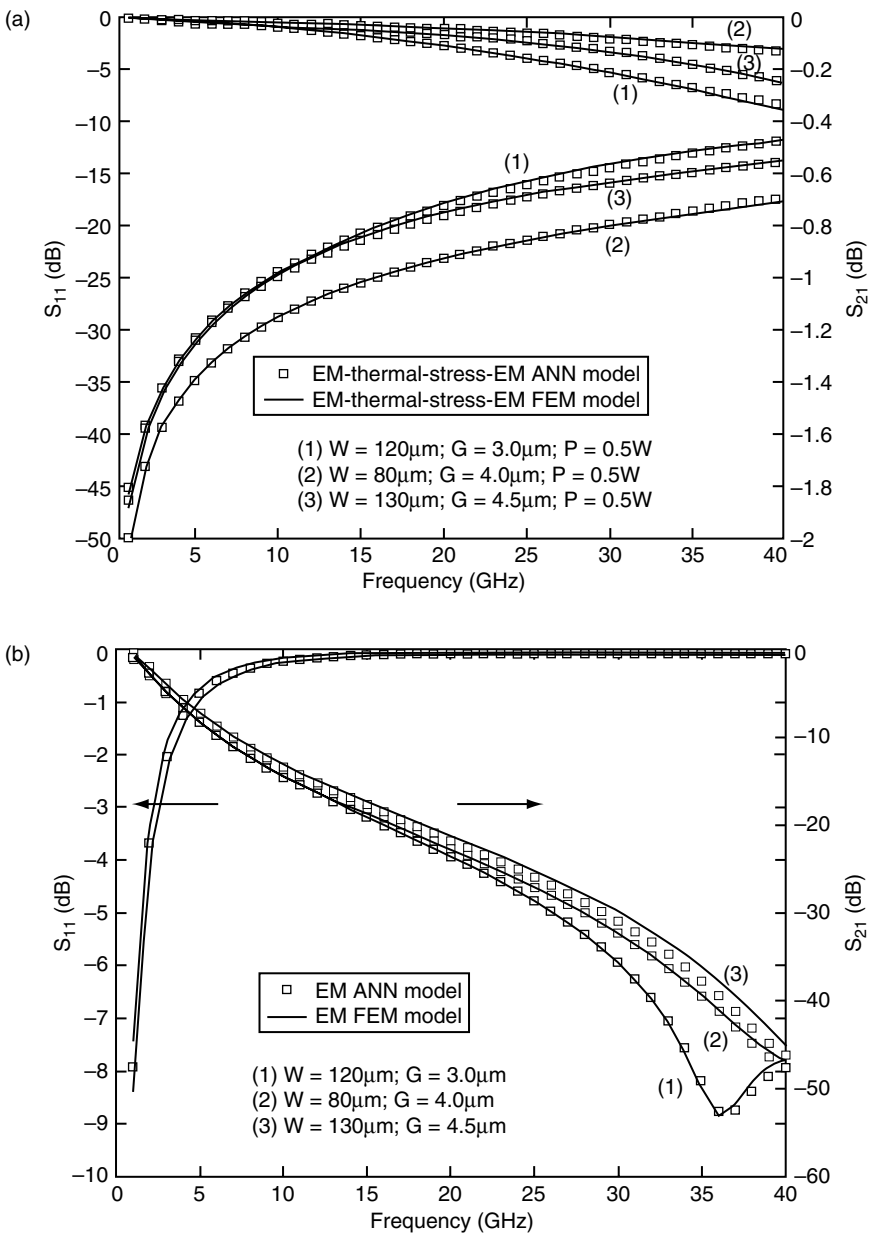

Figure 7 Validation of EM-thermal-stress-EM and EM ANNs with FEM models for the beam in (a) up-state and (b) down-state positions, respectively.

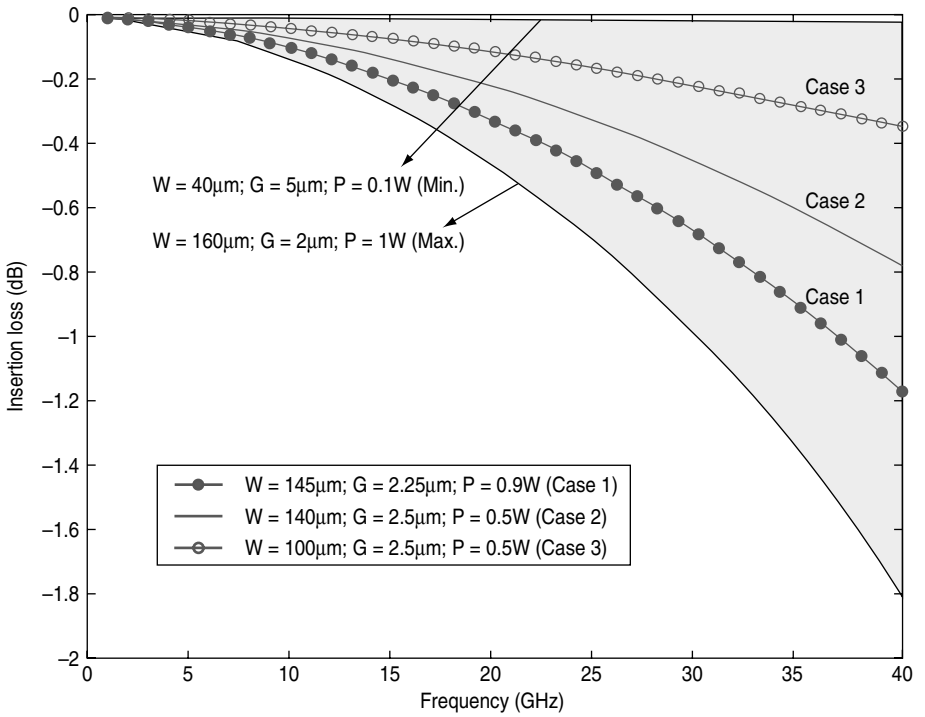

Figure 8 Valid range for insertion loss when the beam is in the up-state position. Nominal performance for the three studied cases is also plotted.

5. SENSITIVITY ANALYSIS

To demonstrate the advantages of the EM-thermal-stress-EM ANN models, we will first determine the most important parameter on the switch RF performance and compare relevant execution times and accuracy. Specifically, the insertion loss sensitivity with respect to the switch width, gap, and RF power is computed. The shaded area in Figure 8 demonstrates the span of insertion loss values within the validity range of ANN model (see Table 2). Three different devices with input parameter variations of ± 10% with respect to initial value are plotted. For the Case 1 with input parameters of W=145μm, G=2.25μm, and P=0.9W, the switch width, W, is varied from 130.5μm (–10%) to 159.5μm (+10%). The remaining parameters are kept unchanged and the corresponding changes of insertion loss at 40GHz are recorded. This frequency is chosen due to the maximum absolute deviation of S-parameters when the multi-physics effects are included in the modeling (see Figure 5). The same procedure is followed for other parameters (gap (G) and power (P)).

Figure 9 summarizes the variation of the insertion loss for the three cases described in Figure 8. The insertion loss is most sensitive to the switch width while it is the least sensitive to the RF power. By performing this study with ANN models, about 1500 times reduced computational time is obtained. Specifically, it took less than 6s with ANN while the execution time for the numerical EM-thermal-stress-EM FEM analysis was about 2hours 25mins. Note that the times needed to transfer the data from one software tool to another were not included in this comparison.

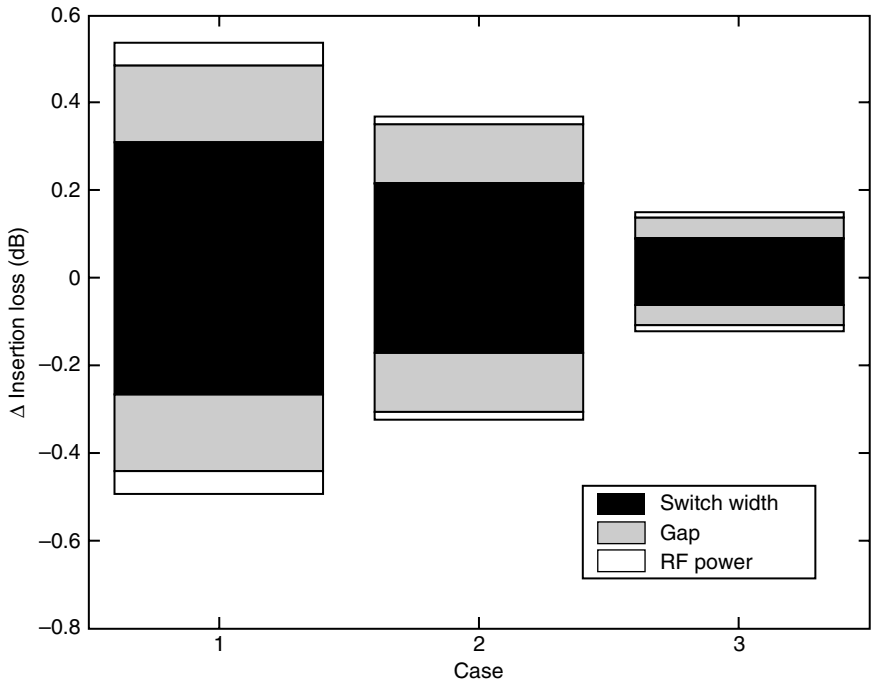

Figure 9 Maximum variations of insertion loss for the three geometries. Each input parameter is changed within a ±10% range from its nominal values.

6. CIRCUIT SIMULATOR INTEGRATION

6.1. INTEGRATION OF THE ANN MODEL

To further demonstrate the advantages and the feasibility of multi-physics computer aided design, the ANN model of the switch is integrated into the circuit simulator, Agilent's ADS [18]. There are several main advantages of this: First, the integrated ANN model is fully compatible with other models of electronic components already existing within the circuit simulator engine. Secondly, the developed EM-thermal-stress-EM model maintains the accuracy of the numerical tools used in their creation. Most importantly, the fast design, analysis and optimization on a device, circuit, and system level with fully compatible multi-physics models of RF MEMS switches are now feasible.

Blackbox modules integration starts with extraction of optimized weight and bias matrices of the ANN model [21]. The input variables are passed to the user-defined model subroutine in the circuit simulator which interfaces the model with the simulator solver engine. The feedforward ANN subroutine reads the models stored as data files and computes the S-parameters. The data file contains the number of inputs, the number of outputs, the number of neurons, weight and bias matrices for each hidden layer. This way, the functionality of the MEMS switch is represented by its ADS library element – a blackbox multi-physics ANN model.

6.2. EXAMPLES: EM-THERMAL-STRESS-EM MEMS SWITCH OPTIMIZATION

Optimization of a switch performance with the developed EM-thermal-stress-EM ANN model is conducted. A schematic with integrated ANN model of a device with the beam

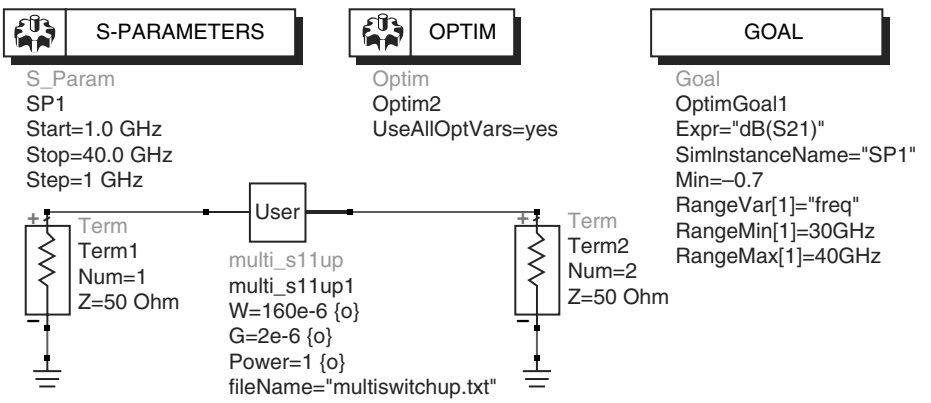

Figure 10 ADS schematic for the optimization setup with integrated multi- physics EM-thermal-stress-EM ANN model.

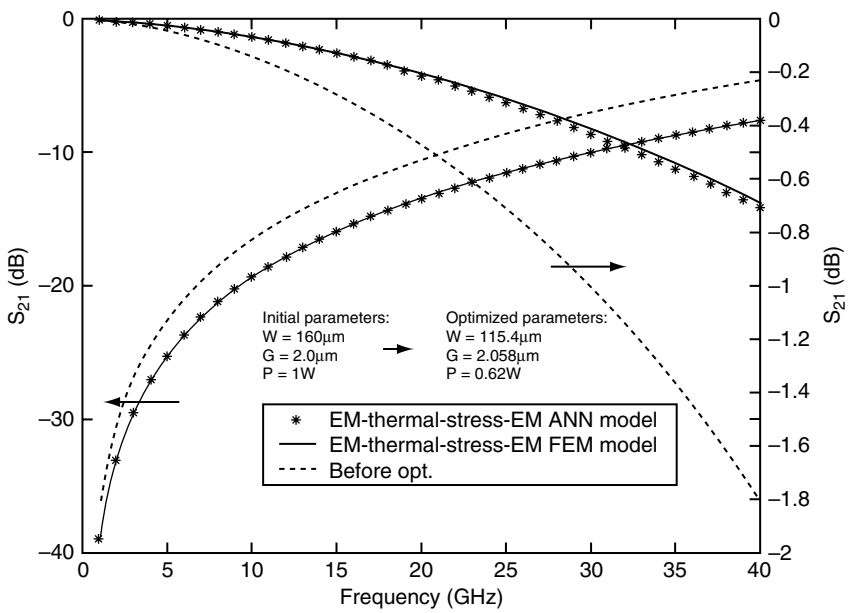

Figure 11 Circuit simulator driven optimization of a shunt switch using developed EM-thermal-stress-EM ANN black-box model and comparison with referenced EM-thermal-stress-EM FEM.

in the up-state position is shown in Figure 10. Note that input variables such as switch width, gap, and RF power are part of schematic and they can be easily controlled by the user. The goal is to find the optimum structural parameters of the device for the insertion loss below 0.7dB throughout 1-40GHz bandwidth. Initial parameters are W=160μm, G=2μm, and P=1W.

The optimization goal is achieved after 11 iterations using gradient method and the results are shown in Figure 11. The optimized input parameters are W=115.4μm, G=2.058μm, and

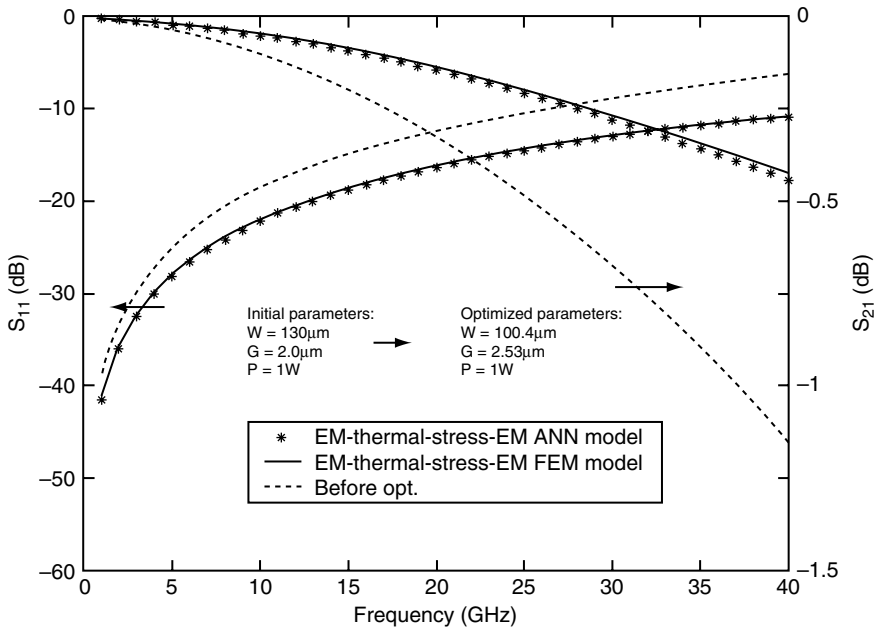

Figure 12 Circuit simulator driven optimization of a shunt switch using developed EM-thermal-stress-EM ANN black-box model and comparison with referenced EM-thermal-stress-EM FEM. Maximum of 1W of power was required in this example.

P=0.62W. To evaluate accuracy of the EM-thermal-stress-EM ANN model, the optimized parameters are used as new inputs for the FEM driven EM, EM-thermal, thermal-stress, and EM simulations. As seen, excellent agreement is maintained. At 40GHz, insertion loss computed in ADS is 0.425dB while HFSS gives 0.442dB. Note that it took only 1.5s for a single run of the multi-physics MEMS switch in ADS compared to ~3mins for a single EM simulation and more than 30mins for multi-physics FEM analysis.

For the second example, the optimization goal is to achieve insertion loss below 0.5dB for maximum of 1W RF power. Initial parameters are W=130μm and G=2.0μm. After 14 iterations using the gradient method, the optimized switch parameters are W=100.4μm and G=2.53μm. As in the previous example, the obtained design parameters are used as input parameters for sequential EM-thermal-stress-EM numerical simulations and obtained results are plotted in Figure 12. Excellent agreement between the EM-thermal-stress-EM circuit model and EM-thermal-stress-EM FEM models is obtained. For a single geometry, it took less than 2s for the EM-thermal-stress-EM ANN model while more than 45mins elapsed for the EM-thermal-stress-EM FEM analysis. As stated earlier, the times needed for manual changes of geometrical set-ups and transitions from one numerical tool (physical domain) to another are excluded from this comparison.

7. DISCUSSION

The development of proposed circuit simulator compatible EM-thermal-stress-EM models is based on an iterative approach composed of sequential solutions in electromagnetic,

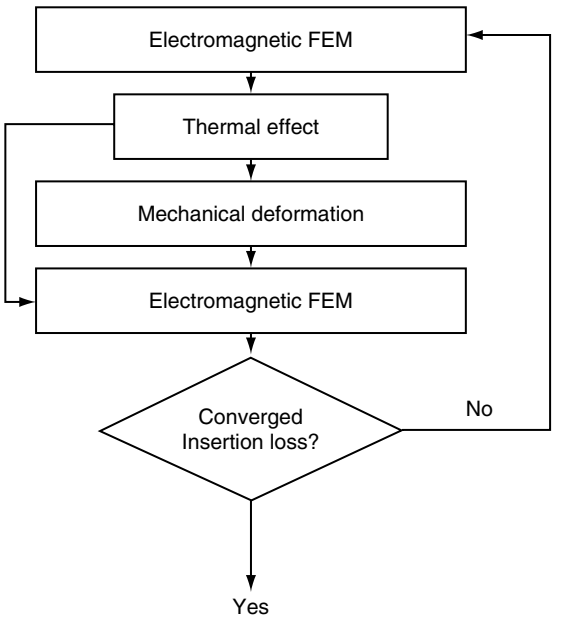

Figure 13 Flow-chart of the iterative EM-thermal-stress-EM FEM analysis used for determining the convergence and accuracy.

thermal, and stress domains. To evaluate its accuracy, the convergence study depicted in Figure 13 is performed.

The power dissipated on the beam is extracted from HFSS and imported to ePhysics. The steady-state temperature on the beam and induced changes in electrical conductivities and beam mechanical deformation are then computed with this tool. Calculated structural deformation profile and conductivity changes are used to update the HFSS model. Finally, execution of the EM analysis, comparison of S-parameters with previous results, and a decision based on the convergence criteria conclude the first iteration. To reduce the time needed to generate multi-physics training datasets for the ANN, the model development here is concluded after the first iteration was completed. Realized accuracy is determined by recording the convergence history for the first seven iterations.

Considered in this section is the case which amounts to the worst accuracy (i.e., the highest thermal-stress effects on S-parameters). Specifically, the beam parameters of W=160μm, G=2μm, and P=1W are chosen. As shown in Figure 14, only 2 iterations are needed for S_{21} to achieve less than 1% difference with the converged value. The beam deformation is also shown to depict that within the studied range, the beam never collapses down. Note that the beam pull down occurs if it deflects to the 2/3 of the initial gap [2]. Based on this criterion, the validity range for the EM-thermal-stress-EM models developed in this paper is given in Table 3. As can be read from the 1st column of the valid range, for the full ranges of the gap (2-5μm), frequency (1-40GHz), and power (0.1-1W), the width of the switch beam should be less than 150μm. As discussed earlier, the relative error after 1st iteration is the worst in this case and it amounts to about 10%. If the training of EM-thermal-stress-EM ANN model would conclude after two iterations, the error associated with the FEM will drop below 0.6%.

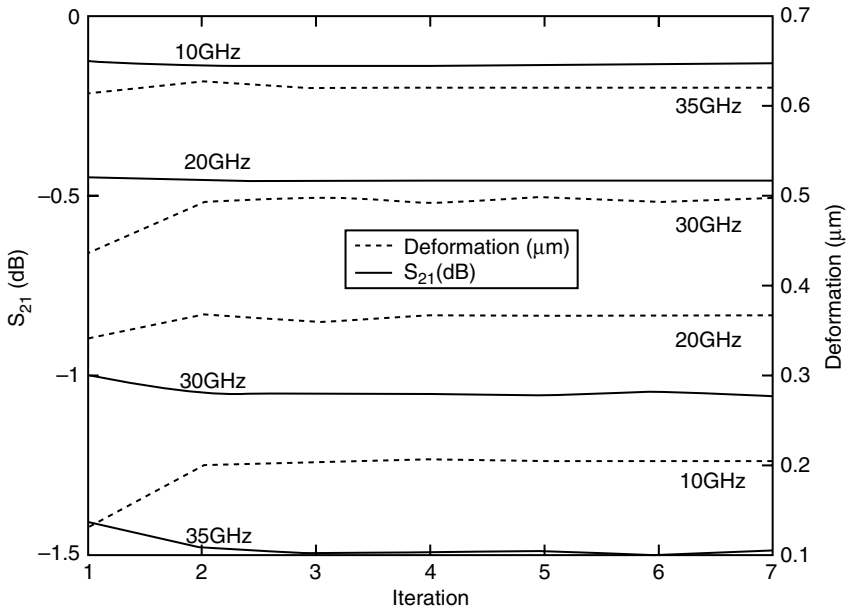

Figure 14 Convergence history of the EM-thermal-stress-EM FEM models. Shown are the insertion loss and beam deformation at 4 frequencies within the valid range of the model.

Table 3 Valid range and max. errors of the developed EM-thermal-stress-EM ANN model

Variables		**Valid range**			**Unit**
Switch width (40~160)	≤150	full	full	full	μm
Gap (2~5)	full	≥2.4	full	full	μm
Frequency (1~40)	full	full	≤35	full	GHz
RF power (0.1~1)	full	full	full	≤0.8	W
Relative error for S21 between 1st and 2nd iteration	10	8	5	3	%

8. SUMMARY

Efficient modeling approach for circuit level multi-physics analysis, design, and optimization of RF MEMS switches using combined FEM and ANN techniques is proposed. A detailed description of all steps and necessary validations are also provided. Several examples clearly demonstrate the advantages that this methodology offers to MEMS designers. Compared to the EM-thermal-stress-EM FEM modeling, the simulation time is reduced for more than 1500 times, yet the accuracy is that of FEM. The system level design and optimization with embedded thermal and stress effects are now feasible. Finally, we note that although demonstrated with a specific RF MEMS device, this methodology is applicable to other devices providing that switch failures are not encountered in any of the physical domains.

REFERENCES

[1] J.B. Muldavin and G.M. Rebeiz, "High- isolation CPW MEMS shunt switches-part 2: design," *IEEE Trans. Microwave Theory and Tech.*, 2000, 48, (6), pp. 1053–1056.

[2] G.M. Rebeiz (Ed.), "RF MEMS theory, design, and technology,"*John Wiley & Sons, Inc*., Hoboken, NJ, USA, 2003.

[3] Steer, M.B *et al,* "Global modeling of spatially distributed microwave and millimeter-wave systems," *IEEE Trans. Microwave. Theory and Technology*, 1999, 47, (6), pp. 830–839.

[4] R.M. Reano, W. Thiel, J.F. Whitaker, and L.P.B. Katehi, "Measured and simulated electric, magnetic, and thermal field distributions of a patch antenna operating at high power," *IEEE Int. Symp Antennas Propagation*, 2002, 2, pp. 886–889.

[5] R.M. Reano, D. Peroulis, and J.F. Whitaker, "Electro/thermal measurements of RF MEMS capacitive switches, " *IEEE MTT-S Digest*, 2003, 3, pp. 1923–1926.

[6] X. Yan, N.E. McGruer, G.G. Adams, and S. Majumder, "Finite element analysis of the thermal characteristics of MEMS switches," *Int. Conf. Solid State Sensors, Actuators and Microsystems*, 2003, Boston, MA, USA, pp. 412–415.

[7] Y. Zhu and H. D. Espinosa, "Effect of temperature on capacitive RF MEMS switch performance-a coupled-field analysis," *J. Micromechanical. Microengineering*, 2004, 14, pp.1270–1279.

[8] P. Robert *et al*, "Integrated RF-MEMS switch based on a combination of thermal and electrostatic actuation," *Int. Conf. Solid State Sensors, Actuators and Microsystem*, 2003, Boston, MA, USA, pp. 1714–1717.

[9] B.D. Jensen, K. Saitou, J.L. Volakis, and K. Kurabayashi, "Fully integrated electrothermal multidomain modeling of RF MEMS switches," *IEEE Microwave and Wireless Components Lett.*, 2003, 13, (9), pp. 364–366.

[10] S.P Kearney, L.M. Phinney, and M.S. Baker, "Spatially resolved temperature mapping of electrothermal actuators by surface Raman scattering," *J. Microelectromech. Syst.*, 2006, 15, pp.314–321.

[11] J.B. Rizk, E. Chaiban, and G.M. Rebeiz, "Steady state thermal analysis and high power reliability considerations of RF MEMS capacitive switches," *IEEE MTT-S Digest*, 2002, Seattle, WA, USA, pp. 239–242.

[12] J. R. Reid, L. A. Starman, and R. T. Webster, "RF actuation of capacitive MEMS switches," *IEEE MTT-S Digest*, 2003, Philadelphia, PA, USA, pp. 1919–1922.

[13] S.D. Senturia (Ed.), "Microsystem design," *Kluer Academic Publishers*, Boston, MA, USA, 2003.

[14] Y. Lee and D.S. Filipovic, "ANN based electromagnetic models for the design of RF MEMS switches," *IEEE Microwave and Wireless Component Lett.*, 2005, 15, pp. 823–825.

[15] J.B. Muldavin and G.M. Rebeiz, "High-isolation CPW MEMS shunt switches. 1. Modeling," *IEEE Trans. Microwave. Theory and Technology.*, 2000, 48, (6), pp. 1045–1052.

[16] Ansoft Inc., High Frequency Structure Simulation (HFSS), Ver. 10, [Online]. Available: http://www.ansoft.com.

[17] Ansoft Inc., ePhysics, Ver. 1, [Online]. Available: http://www.ansoft.com.sg/ePHYSICS.html.

[18] Agilent, Inc., Advanced Design System (ADS), Ver. 2005A, [Online]. Available: http://eesof.tm.agilent.com.

[19] L. Que, J.S. Park, and Y.B. Gianchandani, "Bent-beam electrothermal actuators-Part I: single beam and cascaded devices," *J. Microelectromech. System*. 2001, 10, (2), pp. 247–253.

[20] C. Kittel (Ed.), "Introduction to solid state physics," *John Wiley & Sons, Inc*., New York, NY, USA, 1996.

[21] Y. Lee, Y. Park, F. Niu, and D. Filipovic, "Design and optimization of one-port RF MEMS resonators and related integrated circuits using ANN based macromodeling approach," *IEE Proc. Circuits, Devices and Systems*, 2007, 17, (2), pp.196–209.

[22] Q.J. Zhang and K.C. Gupta (Eds.), "Neural networks for RF and microwave design," Artech House, Norwood, MA, USA, 2000.

ACKNOWLEDGMENT

The authors would like to acknowledge Mr. Brad Brim from Ansoft and Mr. Nilesh Kamdar from Agilent for many useful discussions.